

Introduction

Motivation

As the main source of energy loss in SOFCs, oxygen reduction reaction (ORR) process of LSM based cathode is of great interest. However, the fundamentals such as kinetic mechanism of the ORR remain unclear.

For an in-depth understanding of electrodes, a reaction model involving elementary reaction steps is more suitable than models for global reactions, e.g. Butler-Volmer model.

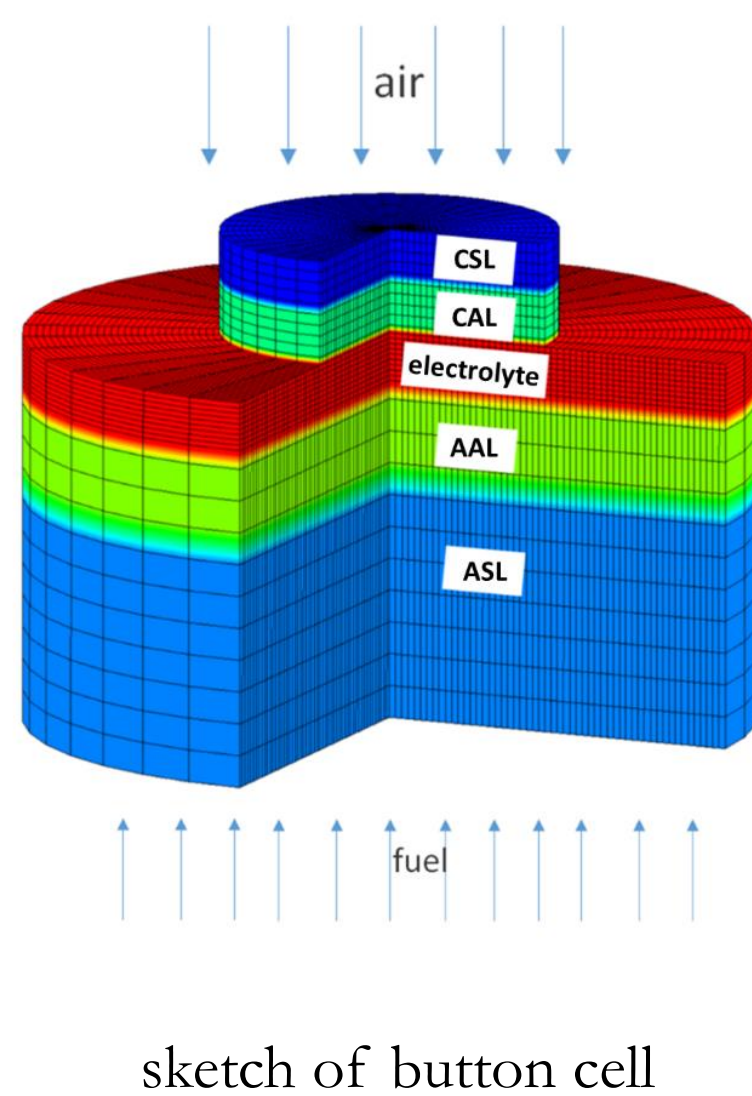
The calibration of multistep ORR mechanism is lacking in the past literature due to the incredible complexity from a large number of parameters.

Purpose of the study

A comprehensive numerical model with parallel pathways for oxygen reduction reaction (ORR) in a composite cathode was developed to gain insights from real solid oxide fuel cell (SOFC) button cell data.

Multi-Physics Modeling

Sketch of button cell model & governing equations



Charge conservation

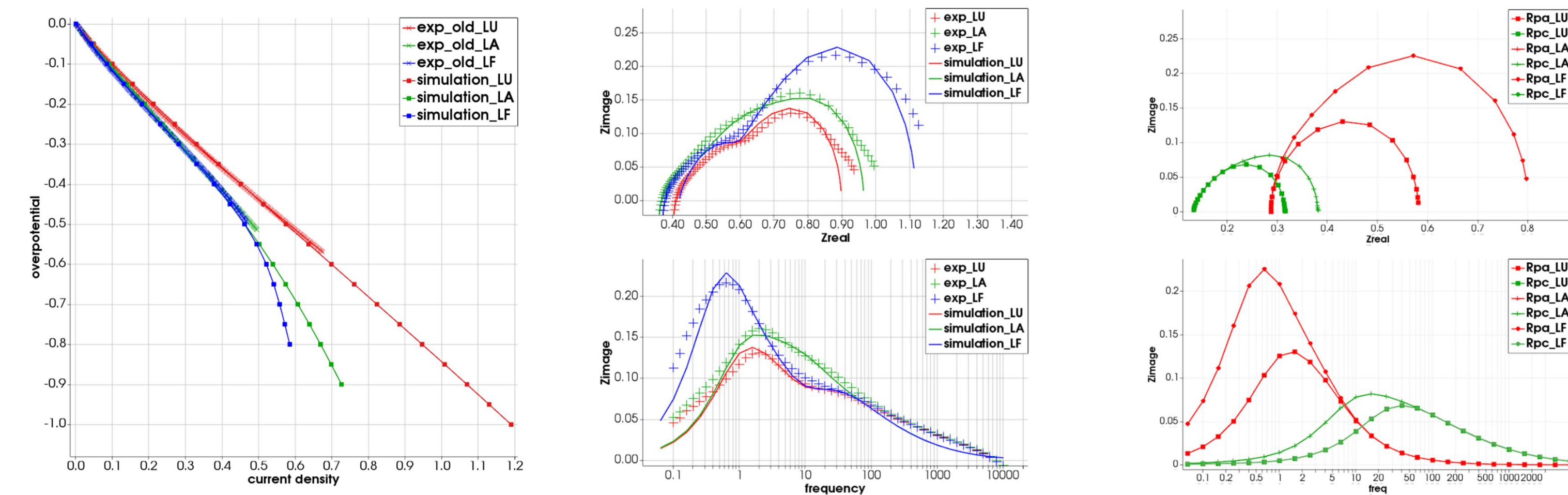
domain	phase	governing equations
Cathode	LSM	$a_{int,c} C_{DL,c} \frac{\partial}{\partial t} (\varphi_c - \varphi_i) + \nabla \cdot (-\sigma_c \nabla \varphi_c) = i_{Fc}$
	YSZ	$a_{int,c} C_{DL,c} \frac{\partial}{\partial t} (\varphi_i - \varphi_c) + \nabla \cdot (-\sigma_i \nabla \varphi_i) = -i_{Fc}$
Electrolyte	YSZ	$\nabla \cdot (-\sigma_i \nabla \varphi_i) = 0$
Anode	YSZ	$a_{int,a} C_{DL,a} \frac{\partial}{\partial t} (\varphi_i - \varphi_a) + \nabla \cdot (-\sigma_i \nabla \varphi_i) = -i_{Fa}$
	Ni	$a_{int,a} C_{DL,a} \frac{\partial}{\partial t} (\varphi_a - \varphi_i) + \nabla \cdot (-\sigma_a \nabla \varphi_a) = i_{Fa}$

Species transportation

$$\varepsilon \frac{\partial \phi}{\partial t} = \nabla \cdot (D_{\phi}^{eff} \nabla \phi) - S_{\phi}$$

Results and Analysis

Calibrated simulations for various air/fuel supply conditions



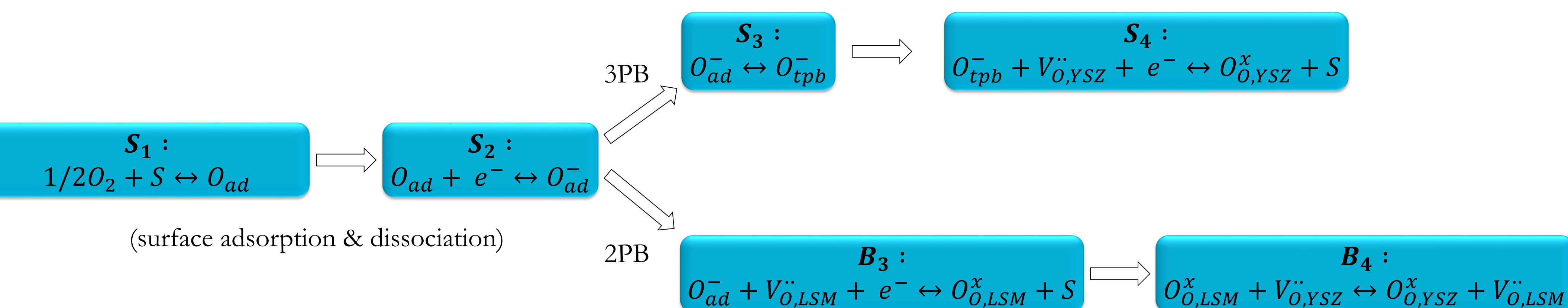
Calibrated V-I curves and impedance behavior for three air/fuel supply conditions and impedance contribution from electrodes

Tuned parameters and comparison to literature results

parameters	variables & unites	present study	literature results
interfacial area between LSM and Pore	$a_{LP} (m^{-1})$	7.414×10^6	$1 \times 10^6 \sim 1 \times 10^7$
interfacial area between LSM and YSZ	$a_{LY} (m^{-1})$	7.414×10^6	$1 \times 10^6 \sim 1 \times 10^7$
double-layer capacitance	$C_{DL,c} (F m^{-2})$	2.975	0.1~27
bulk diffusion coefficient	$D_b (m^2 s^{-1})$	1×10^{-9}	$1 \times 10^{-10} \sim 1 \times 10^{-9}$
surface diffusion coefficient	$D_s (m^2 s^{-1})$	1×10^{-9}	$1 \times 10^{-10} \sim 1 \times 10^{-9}$
density of adsorption sites at LSM/Pore interface	$\Gamma (mol m^{-2})$	1×10^{-5}	$1 \times 10^{-5} \sim 1 \times 10^{-4}$
equilibrium Concentration of adsorbed surface oxygen ion	$C_{O_{eq}} (mol m^{-2})$	3×10^{-6}	$1 \times 10^{-7} \sim 1 \times 10^{-6}$
equilibrium Concentration of adsorbed surface oxygen ion at 3PB	$C_{O_{TPB,eq}} (mol m^{-2})$	3×10^{-7}	
coverage of adsorbed oxygen on LSM	$\theta_{O,eq}$	0.03	0.01 ~ 0.1
equilibrium concentration of oxygen vacancy in LSM	$C_{V,LSM,eq} (mol m^{-3})$	1×10^{-1}	$1 \times 10^{-2} \sim 1 \times 10^{-1}$
equilibrium concentration of oxygen vacancy in YSZ	$C_{V,YSZ,eq} (mol m^{-3})$	5×10^3	
backward rate constants of S1 at reference state	$k_{S1}^{-1} (s^{-1})$	6.002×10^3	
net rate of S2 at reference state	$r_{S2,0} (mol m^{-2} s^{-1})$	3.001×10^{-4}	$1 \times 10^{-4} \sim 1 \times 10^{-3}$
forward rate constants of S3 at reference state	$k_{S3} (s^{-1})$	6.002×10^2	
net rate of S4 at reference state	$r_{S4,0} (mol m^{-2} s^{-1})$	2.5×10^{-3}	1×10^{-2}
net rate of B3 at reference state	$r_{B3,0} (mol m^{-2} s^{-1})$	1.05×10^{-4}	$1 \times 10^{-3} \sim 1 \times 10^{-2}$
net rate of B4 at reference state	$r_{B4,0} (mol m^{-2} s^{-1})$	1×10^{-2}	$1 \times 10^{-3} \sim 1 \times 10^{-2}$

Oxygen Reduction Reaction (ORR) Mechanism

Parallel pathways of ORR mechanism



Reaction rates of elementary steps

$$r_{S1} = k_{S1} \Gamma \theta_s P_{O_2}^{\frac{1}{2}} - k_{S1}^{-1} \Gamma \theta_{Oad}$$

$$r_{S2} = k_{S2} \Gamma \theta_{Oad} \exp(-\alpha f E_s) - k_{S2}^{-1} \Gamma \theta_{Oad}^{-} \exp((1-\alpha) f E_s)$$

$$r_{S3} = k_{S3} \Gamma \theta_{Oad}^{-} - k_{S3}^{-1} \Gamma \theta_{Otpb}^{-}$$

$$r_{S4} = k_{S4} \Gamma \theta_{Otpb}^{-} C_{V,YSZ} \exp(-\alpha f E_s) - k_{S4}^{-1} \Gamma \theta_s \exp((1-\alpha) f E_s)$$

$$r_{B3} = k_{B3} \Gamma \theta_{Oad}^{-} C_{V,LSM} \exp(\alpha f E_b) - k_{B3}^{-1} \Gamma \theta_s (cto - C_{V,LSM}) \exp(-(1-\alpha) f E_b)$$

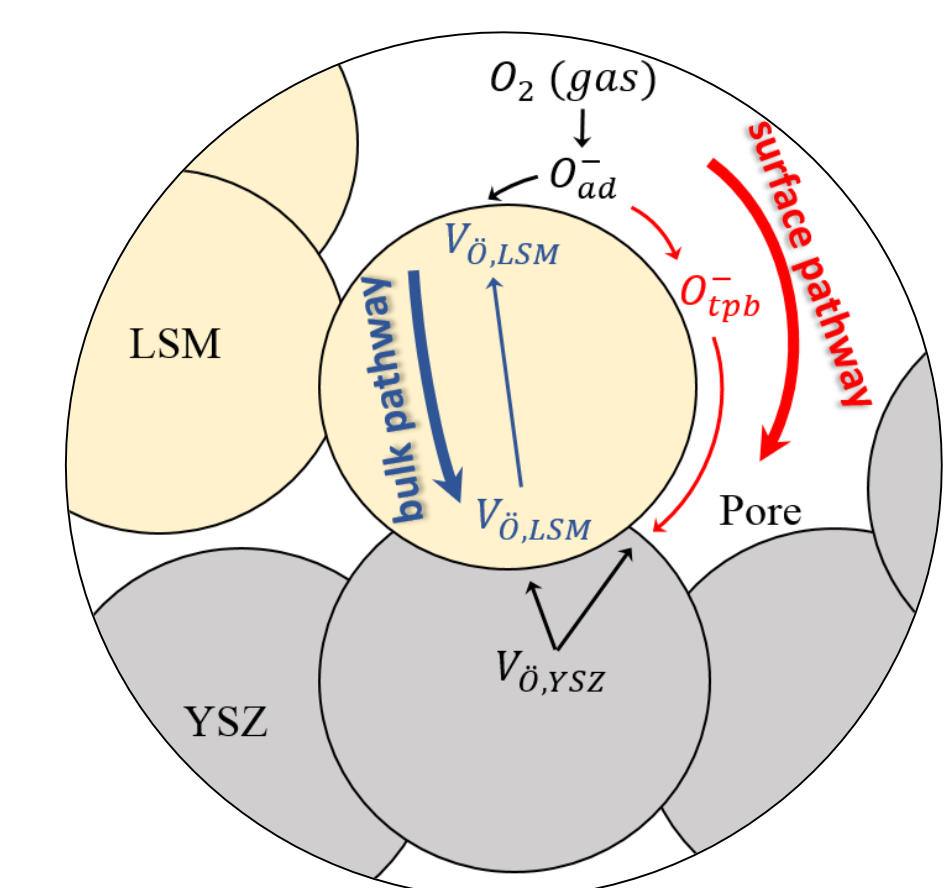
$$r_{B4} = k_{B4} C_{V,YSZ} (cto - C_{V,LSM}) \exp(-2\alpha f E_b) - k_{B4}^{-1} C_{V,LSM} \exp(2(1-\alpha) f E_b)$$

$$r_{S2} \propto P_{O_2}^{3/8}$$

$$r_{S4} \propto P_{O_2}^{1/8}$$

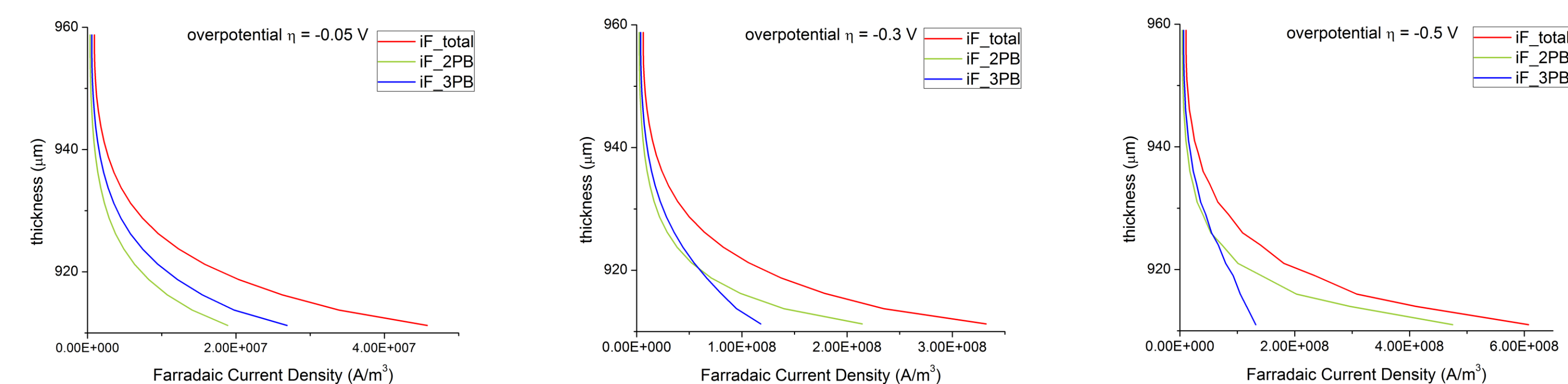
$$r_{B3} \propto P_{O_2}^{-1/8}$$

$$r_{B4} \propto P_{O_2}^{-1/4}$$



sketch of ORR mechanism

Contributions from pathways



3PB and 2PB contributions to the total performance at various operating conditions.

Conclusions

- The calibrated results indicate that surface adsorption and dissociation is the rate-determining step for the cell data under study, which is consistent with the literature findings.
- The overall cell performance can be attributed to the combination of the surface adsorption and dissociation step, charge transfer steps in parallel pathways, and diffusion phenomena.